ELSEVIER

Contents lists available at ScienceDirect

International Journal of Sediment Research

journal homepage: www.elsevier.com/locate/ijsrc



Original Research

A preliminary study of the failure mechanisms of cascading landslide dams

Gordon G.D. Zhou a,b,1, Peng Cui a,b,*, Xinghua Zhu a,b,1, Jinbo Tang a,b,1, Huayong Chen a,b,1, Qicheng Sun c,2

- a Key Laboratory of Mountain Hazards and Earth Surface Process/Institute of Mountain Hazards and Environment, Chinese Academy of Sciences (CAS), Chengdu, China
- ^b CAS Center for Excellence in Tibetan Plateau Earth Sciences
- ^c State Key Laboratory for Hydroscience and Engineering, Tsinghua University, Beijing, China

ARTICLE INFO

Article history:
Received 25 August 2012
Received in revised form
5 September 2014
Accepted 21 September 2014
Available online 1 August 2015

Keywords:
Cascading failure
Landslide dam
Upstream flow
Failure mode
Landscape evolution
Debris flow

ABSTRACT

Landslide dams commonly form when mass earth or rock movements reach a river channel and cause a complete or partial blockage of the channel. Intense rainfalls can induce upstream flows along a sloping channel that significantly affect downstream landslide dams. If a series of landslide dams are collapsed by incoming mountain torrents (induced by intense rainfall), large debris flows can form in a very short period. Furthermore, the failure of these dams can amplify the magnitude and scale of debris flows in the flow direction. The catastrophic debris flows that occurred in Zhouqu County, China on 8 August 2010 were caused by intense rainfall and the upstream cascading failure of landslide dams along the gullies. Incorporating the role of outburst floods associated with the complete or partial failure of landslide dams is an interesting problem usually beyond the scope of analysis because of the inherent modeling complexity. To understand the cascading failure modes of a series of landslide dams, and the dynamic effect these failures have on the enlargement of debris flow scales, experimental tests are conducted in sloping channels mimicking field conditions, with the modeled landslide dams distributed along a sloping channel and crushed by different upstream flows. The failure modes of three different cascades of landslide dams fully or partially blocking a channel river are parametrically studied. This study illustrates that upstream flows can induce a cascading failure of the landslide dams along a channel. Overtopping is the primary failure mechanism, while piping and erosion can also induce failures for different constructed landslide dams. A cascading failure of landslide dams causes a gradually increasing flow velocity and discharge of the front flow, resulting in an increase in both diameter and percentage of the entrained coarse particles. Furthermore, large landslide blockages can act to enhance the efficiency of river incision, or conversely to induce aggradation of fluvial sediments, depending on the blockage factor of the landslide dams and upstream discharge.

© 2015 Published by Elsevier B.V. on behalf of International Research and Training Centre on Erosion and Sedimentation/the World Association for Sedimentation and Erosion Research.

1. Introduction

A landslide that becomes agitated and disaggregated as it tumbles down a steep slope can usually transform into a debris flow if it contains or acquires sufficient water for saturation. Some of the largest and most devastating debris flows originate in this manner (e.g., Plafker & Ericksen, 1978; King et al., 1989; Scott et al., 1995). It has also been widely reported that large landslides can inundate river valleys and overwhelm channels with large volumes of coarse materials, commonly forming stable landslide dams that trigger extensive and prolonged aggradation upstream (Ouimet et al., 2007). Thus, there has been a growing recognition that landsliding exerts a primary control on the planform development, incision history, and sediment discharge of watersheds (Hovius et al., 1997, 1998; Hewitt, 1998; Strasser & Schlunegger, 2005; Korup et al., 2006, 2010; Hsu & Hsu, 2009).

Landslide dams are a very common phenomenon in mountainous areas, forming when a landslide reaches the bottom of a river valley and causes a complete or partial blockage (Ermini & Casagli, 2003). Unlike an artificial gravity or concrete dam with engineered barriers and filter materials, a landslide dam is formed of an unconsolidated heterogeneous mixture of earth or rock debris in a naturally unstable

^{*}Corresponding author at: Key Laboratory of Mountain Hazards and Earth Surface Process/Institute of Mountain Hazards and Environment, Chinese Academy of Sciences (CAS), Chengdu, China. Tel.: + 86 28 85214421; fax: +86 28 85238460.

E-mail addresses: gordon@imde.ac.cn (G.G.D. Zhou), pengcui@imde.ac.cn (P. Cui), zhuxinghua09@163.com (X. Zhu), jinbotang@imde.ac.cn (J. Tang), hychen@imde.ac.cn (H. Chen), qcsun@tsinghua.edu.cn (Q. Sun).

¹ Tel./fax: +86 28 85238460.

² Tel.: +86 10 62796574; fax: +86 10 62773576.

state (Costa, 1985; Li et al., 2011). Freshly deposited landslide soils easily erode, which is a significant factor behind the initiation and development of breaches in landslide dams made from this material (Chang et al., 2011). The longevity of landslide dams depends on many factors, such as rate of inflow into the impoundment, the size and shape of the dam, its geotechnical characteristics, the size of the original landslide deposit (Costa & Schuster, 1988), and the steppool development degree on the spillway of the landslide dam (Wang et al., 2012). Floods arising from the failure of such natural and constructed dams constitute a widespread hazard to people and property, in part due to the suddenness and unpredictability of dam failures of all types (Walder & O'Connor, 1997). The formation and failure of landslide dams are complex processes that occur at the interface between hill slopes and alluvial plain or valley-floor systems on the earth surface.

Understanding, simulating, and predicting the occurrence, longevity, breakdown, and subsequent debris flows of landslide dams have been the focus of a number of different multidiscipline studies (e.g., Costa & Schuster, 1988; Walder & O'Connor, 1997; Li et al., 2002, 2011; Chen et al., 2004; Korup, 2004; Iovine, et al., 2007; Corominas & Moya, 2008; Crosta & Clague, 2009; Dong et al., 2009, 2011; Nandi & Shakoor, 2009; Peng & Zhang, 2012). An important point is that most of these works have only concentrated on the failure of a single landslide dam. However, large earthquakes can cause clusters of landslide dams of multiple types to develop and be distributed close together in canyons (cf. Keefer, 1999; Korup, 2005; Cui et al., 2009). Despite the common occurrence of such phenomena, little attention has been paid to the cascading failure of clusters of landslide dams, which can fail like dominoes along sloping channels.

The catastrophic debris flows that occurred in the county of Zhouqu, in Gansu Province of China, (Aug. 8, 2010) are generally considered to have been induced by upstream flash floods due to intense rainfalls (Yu et al., 2010; Zhao & Cui, 2010; Tang et al., 2011). Before the disaster, the sloping channels of two gullies (Sanyanyu Gully and Luojiayu Gully) were blocked by clusters of landslide dams advancing from side valleys. These landslide dams consisted of almost all of the landslide categories as summarized and illustrated by Costa and Schuster (1988) based on their different orientations with the valley floor. When upland floods moved downwards at high speed and crushed the obstructive landslide dams, the channel blockage was first gradually broken, then followed by a rapid incision. The sediment delivery of the land-

slide debris by the high-speed stream flows was quite large, easily forming debris flows. The flows crossed Zhouqu's urban area, destroying streets, houses, bridges, and causing 1765 deaths. Moreover, the debris flows rushed into the Bailong River, forming a dammed lake about 550 m in length and 70 m in width (across the river), which flooded half of the city. As demonstrated by Tang et al. (2011), the failure of check dams and natural rockfill dams (landslide dams) in the torrent must have contributed to the considerable increase in peak flow discharge (cf. Tang et al., 2011).

After the disaster, there were many collapsed landslide dams of varying degrees along the sloping channel (Fig. 1). There were some large landslide dams with long run-out distances, which may have fully blocked the sloping channel before the debris flow event (Fig. 1a). Meanwhile, many landslide dams and rock dams combined together to fully block the sloping channels (Fig. 1b). These landslide dams were mainly composed of loosely contacted coarse particles that remained quite unstable. In addition to the landslide/rock dams fully blocking the channels, many clusters of other landslide dams only partially blocking the wide sloping channels could be found in the debris flow gullies (Fig. 1c). Based on post-flood field observations, we can postulate a cascading of landslide dam failures caused by upstream flows may

have occurred. A breach of one of the landslide dams may have caused an anomalous flood wave to propagate downstream, inducing more breaches of downstream landslide dams.

This cascading failure effect can significantly amplify the magnitude of the outflow when there are multiple landslide dams distributed along a gully. Moreover, huge amounts of sediment (from the landslide dams and erodible channel beds) can be entrained into the flow to form debris flows. It is likely that large debris flows are due to the conjunction of many landslide dams of different scales (ranging from bank slides to full collapses of a channel wall), bed erosion, and solid transport (Davies, 1986). There are many case studies of individual natural-dam failures (e.g., Costa & Schuster, 1988; Korup, 2002; Korup et al., 2004; Cleary & Prakash, 2004), but an integrated view of the cascading failure of clusters of landslide dams failing like dominoes along slope channels does not exist. The mechanisms behind the cascading failure of different types of landslide dams are still not clear.

To understand this important natural process, we conducted physical experiments to systematically investigate the failure mechanisms of different cascading landslide dams caused by upstream flows. By analyzing the results from these experiments, this paper aims to infer the failure modes and the evolution of natural cascading landslide dams of different types and simulate those failure modes in modeled experiments.

2. Experimental method

2.1. Test site and soil properties of landslide dams

All experiments were conducted in the Jiangjia Ravine and on a debris fan of the Chaqing Gully, which are located near the Dongchuan Debris Flow Observation and Research Station (DDFORS) (Fig. 2), in the Dongchuan District, Yunnan Province of China (N26°14′, E103°08′). In previous years, most debris flows occurring in the Chaqing Gully and in the Jiangjia Ravine deposited on the fans with an inclined angle of approximately 6° and 4°, respectively. Fig. 3 shows the modeled sloping channels constructed on the floodplain of the Jiangjia Ravine and on the debris fan of the Chaqing Gully. To simulate the cascading failures of large landslide dams that fully block sloping channels, two model tests (No. 1 and No. 2) were conducted on the floodplain of the Jiangjia Ravine. The length of the channel was 15 m long, with a rectangular cross section 1.0 m wide and 0.5 m deep. A third model test (No. 3) was conducted on the deposition fan of the Chaqing Gully to take into account the failures of landslide dams triggered by local rock avalanches or collapses that only partially block sloping channels. The channel was 15 m long, with a rectangular cross section 0.5 m wide and 0.7 m deep. Local farmers had previously excavated a relatively straight aqueduct for irrigation that stretched from the main channel of the Jiangjia Ravine to downstream farmlands. This aqueduct was used to direct the sediment flows from the Jiangjia Ravine to the artificial sloping channel (Test No. 3) for modeling upstream flows, and to crush the downstream landslide dams distributed along the two banks of the channel. The sediment flows in the aqueduct move gently as the declination of the channel bed is guite small, which means discharge Q_0 can be controlled and kept relatively constant (Fig. 3). The densities of the sediment flows in the three modeling tests were measured to be about 1050 kg m^{-3} .

To clarify the processes involved in landslide dam failure, and to provide information on the effect of upstream flows and cascading landslide dam failures on the likely downstream peak discharge, we also constructed physical models of the rock/landslide dams. These dams were designed to be dynamically similar to the rock/landslide dams found in Zhouqu using similarity theory (Yalin, 1971). To emulate the poorly sorted soil properties of existing landslide dams, and to sufficiently reproduce the grain-size distribution in the models,

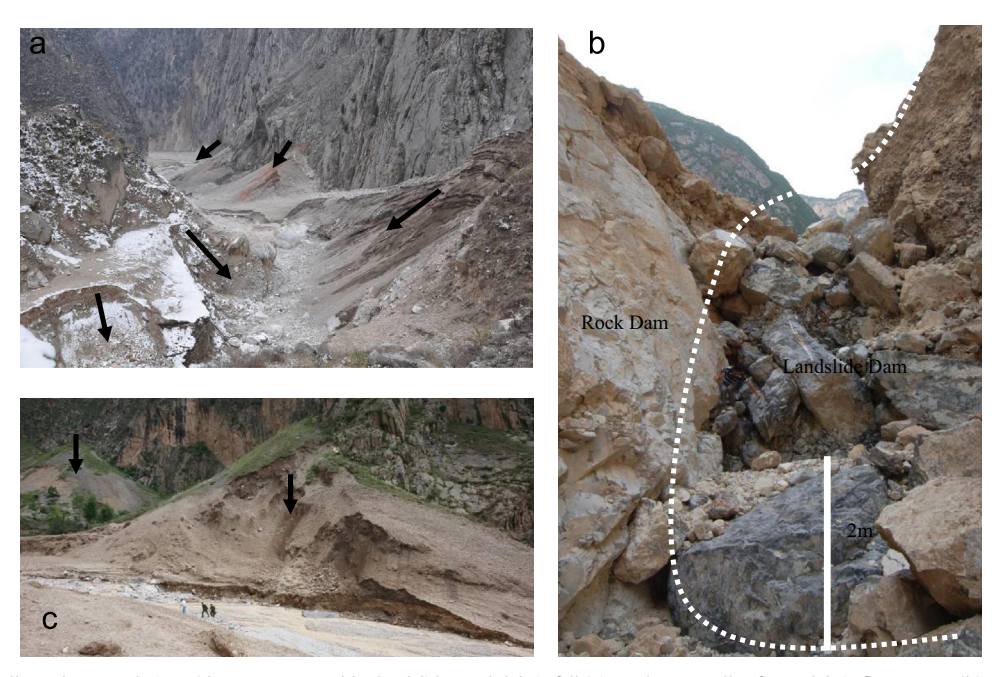


Fig. 1. (a) A cluster of collapsed accumulations (dams constructed by landslides and debris falls) in a Zhouqu gully after a debris flow event; (b) a narrow sloping channel fully blocked by a landslide dam and a rock dam; (c) a wide sloping channel partially blocked by a cluster of landslide dams. Arrows in (a) and (c) depict the failure direction of the landslide dams by upstream flows; photographs (b) and (c) courtesy of Dr. Y. G. Ge.

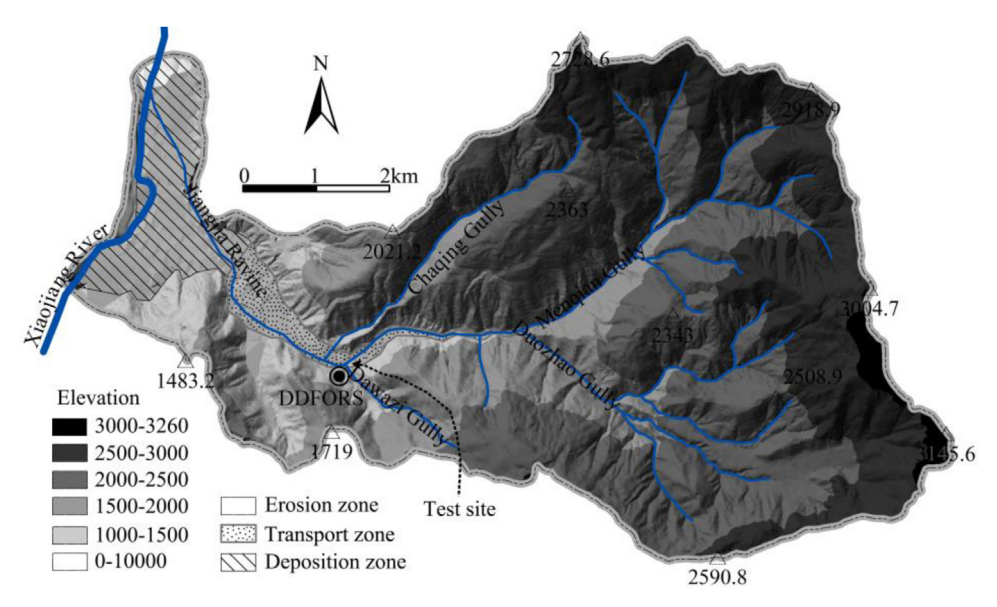


Fig. 2. Elevation profiles of the Jiangjia Ravine and the test site; the numbers are elevation in meters above sea level.

granular materials from the debris fan itself were used to construct the modeled landslide dams (Fig. 3). For particles > 0.25 mm, the grain-size distributions of the granular soil were measured by dry sieving. For those fine particles passing the 0.25 mm sieve, particle size was measured with a Malvern instrument in the laboratory of DDFORS (Dongchuan Debris Flow Observation and Research Station). Fig. 4 shows the grain-size distributions of the modeled landslide dams, which are quite similar to the field landslide soils found in Zhouqu. To simulate typical unconsolidated landslide soils that occur in a naturally unstable state, the granular material from the debris fan was directly poured into the channel without any consolidation process to form the landslide dams. The void ratios of the modeled landslide dams were mostly in the range of 0.5–0.6, a value consistent with the void ratios found in existing landslide dams in Zhouqu.

2.2. Instrumentation and experimental testing procedures

We conducted three experimental tests on the debris fans to observe cascading failures of landslide dams along sloping channels caused by different upstream flows. All of the model scales of the landslide dams, discharge of upstream flow, and other experiment details can be found in Table 1.

The three model tests each considered a different series of landslide dams in the Zhouqu debris flow gullies, with each setup influenced by different upstream flows and the different geomorphologic properties of the canyons. For Test No. 1, six landslide dams fully blocking the sloping channel were constructed and distributed along the channel banks (Fig. 5a). To ensure similarity with real-world situations and for better comparison, a modeled

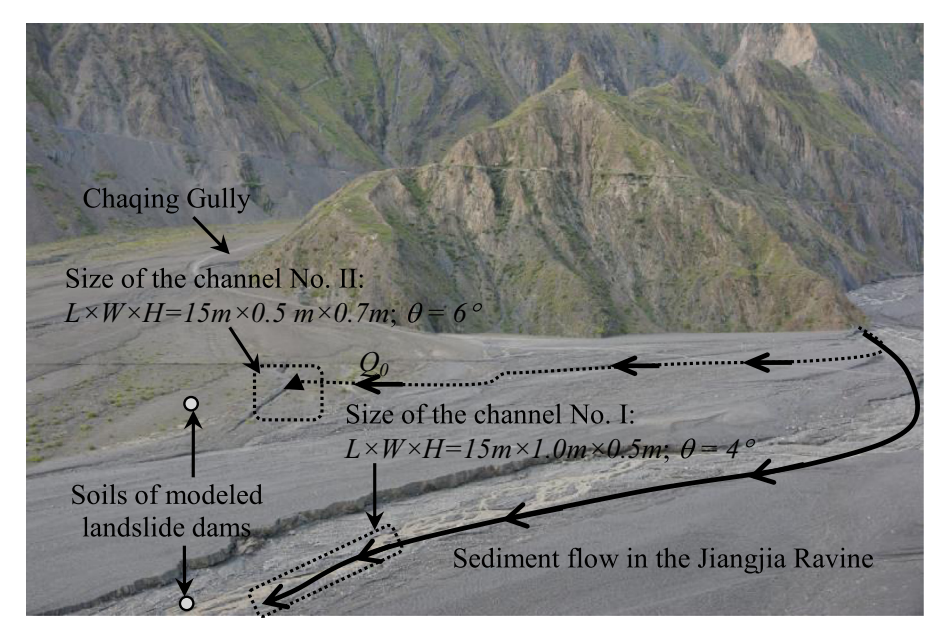


Fig. 3. Location of the test sites in the Jiangjia Ravine and on the debris fan of the Chaqing Gully.

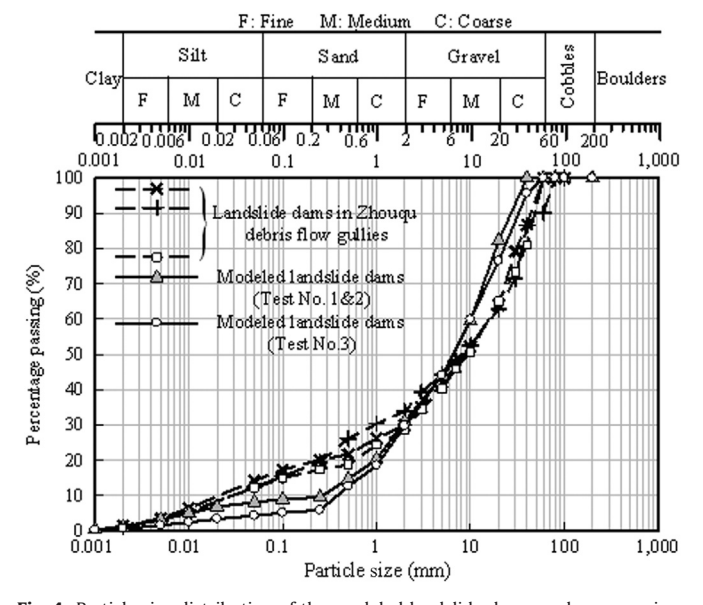


Fig. 4. Particle size distribution of the modeled landslide dams, and a comparison with field particle size conditions.

rock dam was also constructed to form a shallow cross-section with landslide dam No. 4. Upstream sediment flows Q₀ from the Jiangjia Ravine were kept to a relatively small constant value so as to crush the landslide dams with low velocities. As shown in Fig. 5a, two video cameras were installed on the channel banks to record the entire flow process. The front head of the flow was captured by the video cameras, allowing us to estimate the front velocity U of the flow. The front flows that breached each successive landslide dam and crossed different sections were sampled, with the samples marked as A, D, and G. Surveying rods (rulers) were installed along the sloping channel and beside the landslide dams at different sections which, together with the video cameras, were used to determine the thickness h of the flows. These results were subsequently recorded for analysis. We then used these measurements to calculate the front discharge Q from $Q = k \times U \times W \times h$, where W is the channel width. Considering that the front head of the descending flow is a little bit from the main body (not uniformly distributed) and most of the

cross-sections of natural sloping channels are not formed like a rectangular, a coefficient k is needed to multiple. Just for simplicity and focus on the analysis, the value of k is mostly taken to be 1.

Similar to the model setup of Test No. 1, six landslide dams were constructed and distributed along the same sloping channel for Test No. 2 (see Fig. 5b). Large landslide dams with long run-out distances, such as those modeled in Test No. 1, can initially fully block sloping channels. However, landslides of comparatively smaller magnitude usually possess limited flow speeds and few actually reach the opposite bank. Thus, under most conditions, landslide dams are deposited aside the channel bank and only partially block sloping channels in a flow's initial stages. However, when multiple rock avalanches or collapses occur in a channel and result in the development of relatively stable rock dams, the sloping channel can potentially be fully blocked by a conjunction of landslide and rock dams, as occurred in the Zhouqu debris flow gullies. In many of the gullies, a number of cascading landslide dams were distributed along the channel and formed shallow cross-sections with rock dams (Fig. 1b). Such conditions were modeled by Test No. 2, where five landslide dams were constructed using granular materials from the floodplain. In addition to these landslide dams, large boulders were piled up to form stable rock dams (Fig. 5b). The structure of the modeled channel for Test No. 2 was quite similar to alluvial step-pools, which are believed to stabilize riverbeds. Two video cameras and several surveying rods were installed on the channel banks to capture breaches of the landslide dams, observe the front flows, and record the whole flow process. Similar to Test No. 1, the front flows that breached the landslide dams and crossed different sections were sampled and marked as A. D. and G.

Test No. 3 was different from the conditions of Tests No. 1 and No. 2, with interleaved cascading landslide dams distributed along a curved channel used for the field investigation. Those landslide dams partially blocked the sloping channel, and then were mostly crushed by upland flash floods with high velocities. To simulate this situation, five cascading landslide dams were constructed and distributed along a relatively curved channel (Fig. 5c). As in Tests No. 1 and No. 2, video cameras and surveying rods were installed to capture images of the front head and to estimate the flow discharge during the test. To analyze the solids entrained by the flows, we sampled the front flows that breached the landslide dams and crossed different sections. These samples are marked as A, D, and F in Fig. 5c. Furthermore, the geomorphology of the sloping channel was depicted and recorded by a 3D laser scanner

 Table 1

 Characteristics of the prototype and modeled landslide dams.

Sloping Channel No.	Test No.	Characteristics of cascading landslide dams	Prototype sizes of landslide dams in Zhouqu debris flow gullies			$\lambda_L = \frac{L_p}{L_m}$	Sizes of the modeled landslide dams			Initial upstream discharge Q ₀ (m ³ /s)
			Dam No.	<i>L</i> _p (m)	<i>W</i> _p (m)		L_m (m)	<i>H_m</i> (m)	<i>W</i> _m (m)	•
I	1	Large landslide dams fully block the sloping channel: Landslide dam	1 2 3 4 5 6	25 20 15 12 9 6	12 40 9 40 12 36 9 30 6 27 6 15	30	0.8 0.7 0.5 0.4 0.3 0.2	0.4 0.3 0.4 0.3 0.2 0.2	1.3 1.3 1.2 1.0 0.9 0.5	0.025
	2	Landslide dams fully block the sloping chan with rock dams: Rock dam Landslide dam	1 2 3 4 5 6	19 19 18 16 13 18	13 30 11 43 16 42 12 31 12 35 13 32	30	0.6 0.6 0.5 0.4 0.6	0.4 0.4 0.5 0.4 0.4	1.0 1.4 1.4 1.0 1.2 1.0	0.025
п	3	Landslide dams partially block the sloping channel and stand aside banks: Landslide dams Channel side wall Landslide dam	1 2 3 4 5	90 95 78 76 82	40 46 37 47 40 49 35 48 40 50	90	1.0 1.0 0.8 0.8 0.8	0.4 0.4 0.4 0.4 0.4	0.5 0.5 0.5 0.5 0.5	0.01
		Upstream flow Stoping channel								

before and after the test in order to analyze any erosion and aggradation of the channel bed resulting from the flow discharge.

3. Results and discussion

3.1. Cascading failure of landslide dams due to overtopping

Three failure mechanisms are typically the cause of instability and failure of landslide dams: overtopping, piping, and slope failure (Costa & Schuster, 1988; Swanson et al., 1986). Overtopping is usually considered to be the most important of these failure modes (Costa & Schuster, 1988; Dong et al., 2011).

Experimental Test No. 1 used a comparatively low flow discharge (0.025 m³/s), with the upstream flow descending along sloping channel I with a very low velocity (about 0.5 m/s). Initially, the flow interacts with the first landslide dam, as seen in Fig. 6a. At this point, most of the incoming fluid is obstructed and accumulates upstream of the fill except for a small amount of water that penetrates through the soil voids of the landslide dam. The water level of the impoundment continuously increases behind landslide dam No. 1 until the flow overtops the crest of the dam. A large breach starts at the crest, the center point of the dam margin. As the fluid escapes through the breach, the flow gradually erodes soil particles from the dam and gently entrains them into the flow. This process rapidly widens the breaches inside the dam body and

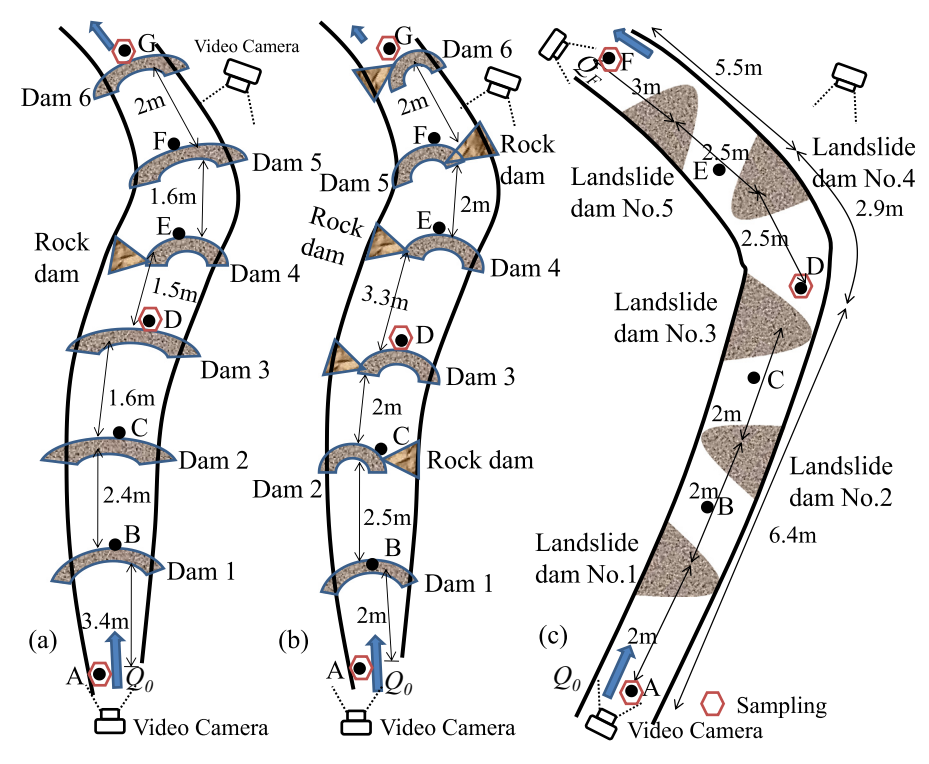


Fig. 5. Schematic diagram of the experimental setup: (a) model Test No. 1; (b) model Test No. 2; and (c) model Test No. 3.

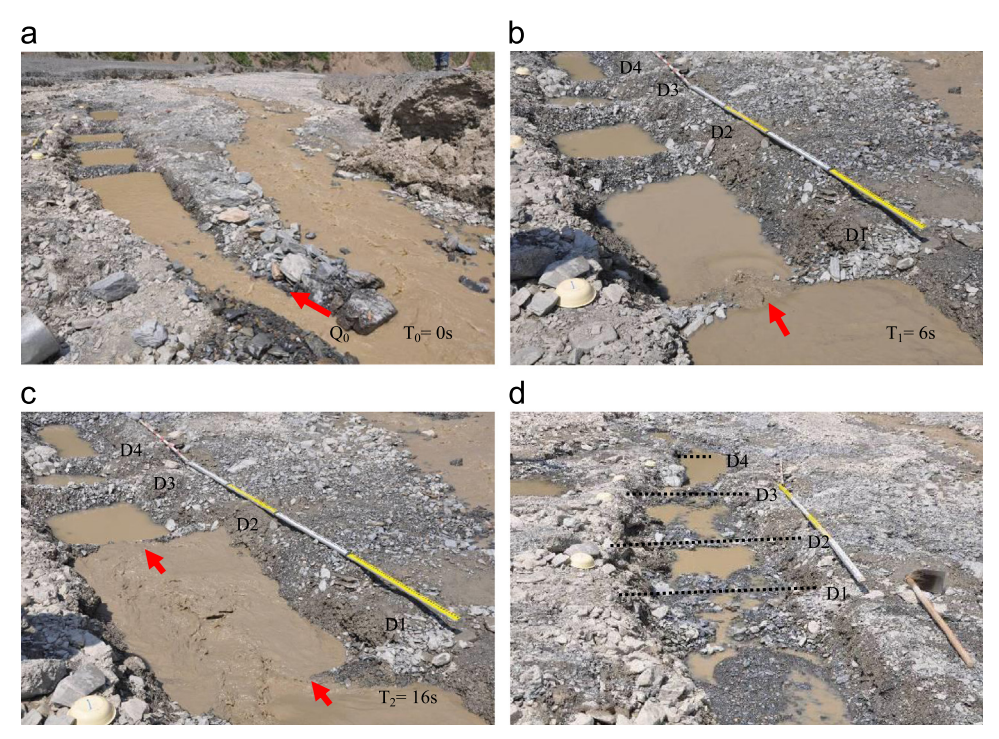


Fig. 6. Evolution of the failure process of the soil dams in model Test No. 1.

causes further collapse/failure of the landslide dam (Fig. 6a and b). After the collapse of landslide dam No. 1, a rapid downward flow develops from the dam crest to the dam toe (point "a" to point "b" in Fig. 7). After a period of acceleration (the process from "b" to "c" in Fig. 7), the front flow is obstructed by the second landslide dam, which quickly raises the water levels behind the dams (cf. Fig. 6b and c). As illustrated in Fig. 7, the front velocity passing through the toe to the crest of landslide dam No. 2 (i.e., from point "c" to point "d" in Fig. 7) sharply decreases. However, once the second

dam failure occurs, a strong wave immediately forms and accelerates along the sloping channel (from point "d" to point "f" in Fig. 7). This process repeats for each successive landslide dam, and downstream debris flows gradually develop with increased flow velocities/discharges (see the peak values in Fig. 7) in a sequence of cascading failures at consecutive downstream landslide dams.

The recorded video provides more detail of the cascading landslide dam failures, showing the overtopping flows above the crests of the landslide dams and of the further inundation of the

sloping channel. Analysis of the video supports the reasonable simplifying assumption that the only part of the breach-opening process of hydraulic importance for each dam failure is widening by erosion. The water level at the back of the dam (i.e., the upstream face) gradually increases, and more and more solidswater mixtures accumulate there to form a dammed lake. Because of this increasing water head, more and more bank soils lose shear strength and collapse inside the dammed lake. Rather than the immediate collapse that can occur as a result of crushing upstream flows, landslide dams that fully block a channel river mostly fail because of successive overtopping. The residual dams along the sloping channel in Fig. 6d further illustrate that most of the upstream landslide dams (from No. 1 to No. 4) were only partially damaged by flows (i.e., residual soils from the landslide dams can be found), rather than completely collapsing like the two downstream landslide dams (No. 5 and No. 6). Moreover, large quantities of coarse sediments were found deposited before the partially collapsed landslide dams (from No. 1 to No. 4) due to

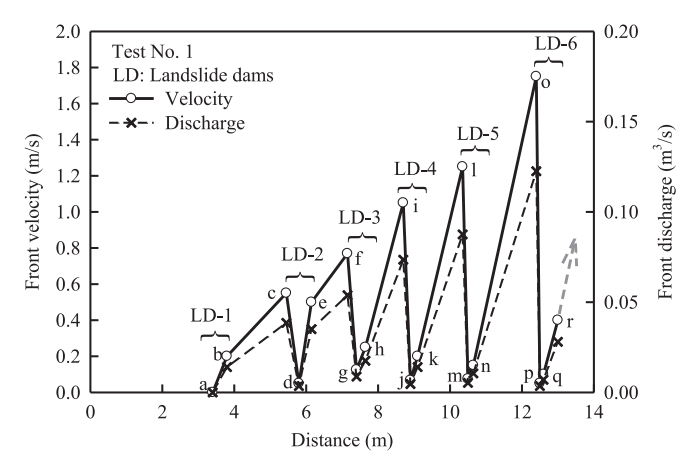


Fig. 7. Variation in the measured velocity and discharge of the front debris flow along the sloping channel for Test No. 1.

the limited upstream flow discharge and velocity. This also proves that the flow discharge and impact energy gradually increase due to the cascading failure of landslide dams. Such successively enlarged flow scales can become a significant threat to downstream communities and populations. The resulting granular aggradation and uplifted channel bed further reflect the fact that the failures of landslide dams in canyons also exert a significant influence on local geomorphology evolution.

3.2. Cascading failure of landslide dams due to overtopping and piping

For experimental Test No. 2, we first constructed a soil dam (dam No. 1) to fully block the sloping channel. Such a soil dam can accumulate large amounts of fluid and energy behind it from upstream flows. When the soil dam fails, the constrained upstream flow immediately pours out with sufficiently high velocity that the flow crushes the downstream landslide dams, even though the upstream flow discharge remained the same as in model Test No. 1 (cf. Table 1). The other five well constructed landslide dams consisted of piled up large boulders and cobbles that fully blocked the channel with rock dams (Fig. 8a). This system of cascading landslide/rock dams is nominally quite similar to an alluvial step-pool. Note that such step-pools usually play an important role in stabilizing a riverbed by dissipating a significant amount of vibrational energy (cf. Wang & Zhang, 2012). However, the system of dams in Test No. 2 was different from typical alluvial steps in that such alluvial steps are usually made of coarse boulders and remain stable (i.e., good shock resistance) towards the upstream flows, whereas the initial landslide dam in the sloping channel in Test No. 2 was easily crushed and eroded by rapid flows. Note that the cascading failure of the landslide dams occurs quite rapidly (Fig. 8b and c). The failure mode of the dams in Test No. 2 is similar to the one observed in model Test No. 1 in that the descending upstream flow raised the water levels behind the landslide dams, allowing the flow to overtop the crests of the landslide dams at the edges of the rock dams. These breaches were

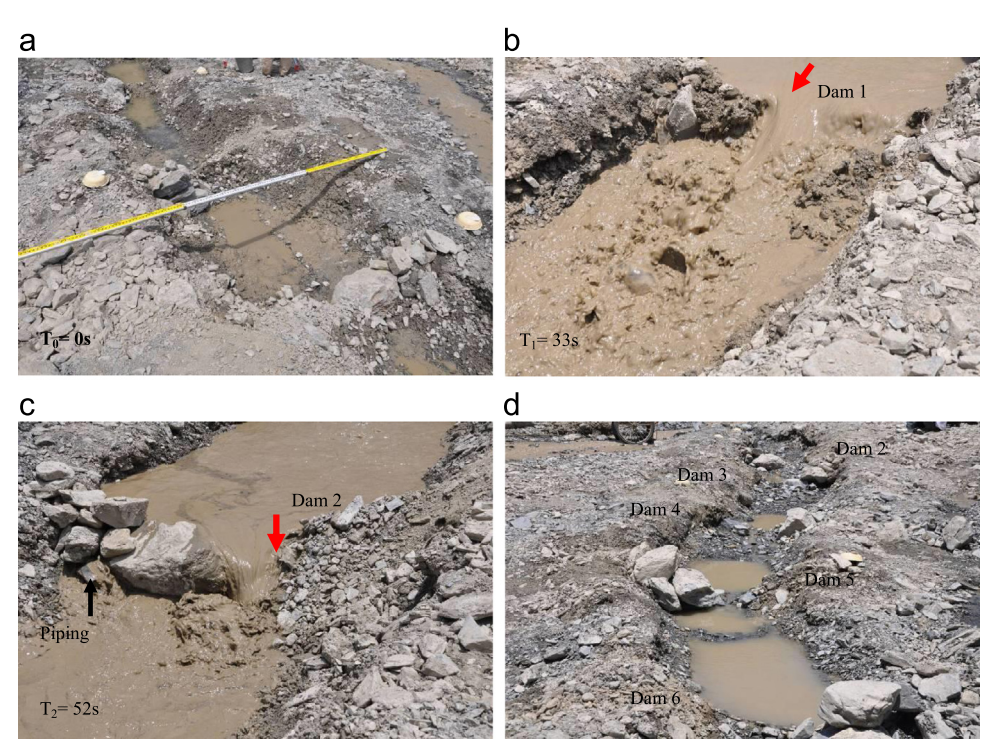


Fig. 8. Evolution of the failure process of the soil dams in model Test No. 2.

continuously widened by flows, and the solids of the landslide dams gradually eroded and entrained into the flows. Rapid flows triggered by the collapse of each landslide dam transported downwards and induced further dam failures like falling dominos. The measured variation in the front velocity and discharge at each of the cascading landslide dam failures is shown in Fig. 9, and is quite similar to the velocities and discharges measured in model Test No. 1.

This process of landslide dam breach formation involving both tractive erosion of sediment, particularly in the early stages of breach formation as water flows over the downstream face of the dam, and the collapse of large masses of sediment that are subsequently entrained and removed by the flowing water (Walder & O'Connor, 1997) is consistent with field observations of actual earthen-dam failures (e.g., Ralston, 1987). Two erosional processes are assumed to operate more or less sequentially during the formation and widening of a breach. First, the upstream sediment wedge collapses into the initial breach, and the floodwaters remove that sediment at a rate determined by the characteristics of the flow. Once the collapsed sediments have been removed, the flood waters erode the breach floor at a rate controlled by the flood's bed load-transport capacity, assuming that the suspended-sediment transport is negligible (cf. Walder & O'Connor, 1997). Once all sediments are removed as bed load, we must relate the bed load flux to the discharge through the breach. The volumetric bed load flux per unit width (or "bed-load transport rates) is generally considered a nonlinear function of the difference between the effective basal shear stress τ' and the critical shear stress τ_c required to initiate transport (cf. Montgomery et al., 1999)

$$Q_S = k(\tau' - \tau_c)^{\lambda} \tag{1}$$

where Q_S is the sediment flux, k is an empirical constant, and λ is an empirically derived exponent generally greater than one (Gomez & Church, 1989). The simplest method for calculating the effective basal shear stress τ' in Eq. (1) for an unsteady flow is to utilize direct measurements of the friction velocity U_* (Carrivick, 2010)

$$\tau' = \rho U_*^2 \tag{2}$$

where ρ is the fluid density. Nezu et al. (1997) gave an overview of five different methods for calculating the friction velocity, and also determined that U_* can be estimated from the depth-averaged velocity \overline{U} (cf. Richardson et al., 1990; Julien, 1995). Montgomery et al. (1999) further demonstrated that a force balance for the moments acting about a downstream contact point for spherical grains of diameter D shows that the critical shear stress, τ_c , required to mobilize a stream bed is proportional to both D and the friction

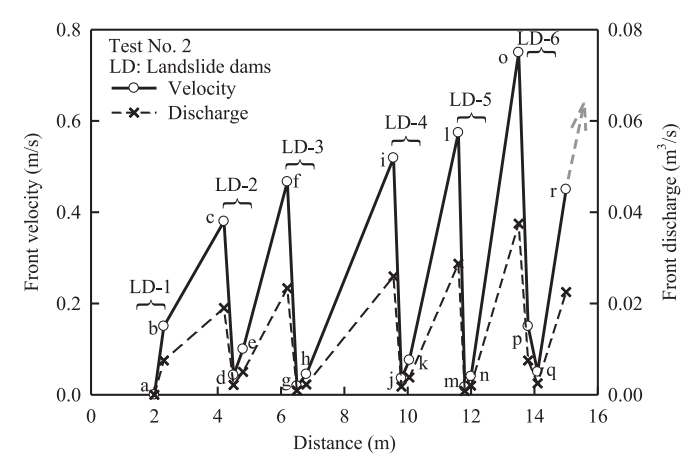


Fig. 9. Variation in the measured velocity and discharge of the front debris flow along the sloping channel for Test No. 2.

angle ϕ' of the bed material and inversely proportional to grain protrusion P. However, because P and ϕ' distributions are difficult to quantify in natural channels, researchers introduced an empirical value τ_c^* to account for these factors where τ_c is generally modeled by the Shields (1936) equation

$$\tau_{c} = \tau_{c}^{*}(\rho_{s} - \rho_{w})gD \tag{3}$$

where ρ_s and ρ_w are the density of sediment and water, respectively, and g is gravitational acceleration. Based on Eqs. (1) and (3), it is apparent that a uniform fining of the bed surface (i.e., a smaller D) decreases τ_c , which leads to increased sediment transport. Similarly, an increase in τ' -through, for example, decreased bed roughness (and which accounts for the increased flow velocity in Eq. (2))—should also increase sediment transport (Montgomery et al., 1999).

Fig. 10 shows the various particle sizes entrained in the front flows, determined by sampling at three different locations along the sloping channel (A, D, and G in Fig. 5a and b). The results illustrate how the cascading landslide dam failures result in more and more relatively fine grains from the collapsed soils become eroded and entrained by the front flow along the sloping channel (cf. the granular materials of the model landslide dams and the particles in sampled flows in Fig. 10). Furthermore, the mean particle diameter (d_{50}) of the descending flows also gradually increases because of the dependence of soil erodibility on flow velocity (cf. Eqs. (1)-(3)) and the measured increase in front velocity recorded after successive dam failures. Moreover, coarse particles in the collapsed landslide dams in model Test No. 2 were mostly deposited beneath the water table and along the downstream face of the originally constructed landslide dams by the flow. Wilcox and Wohl (2007) illustrated that the physical basis explaining the results from many research works (e.g., Thompson et al., 1998) is most likely a flow deceleration in scour pools downstream of steps; thus a large quantity of sediments deposit inside such pools (cf. Chartrand et al., 2011). This model also helps to explain the stabilization of riverbeds caused by step-pool systems. However, rapid piping beneath the rock dams is also clearly observed in Fig. 8c, working in conjunction with the cascading failures of the landslide dams. Because the voids are definitely large in rock dams mainly constructed by boulders and cobbles, many porous media can easily percolate through the pore space with little energy dissipated. This means that the piping water flows that develop from burst upstream landslide dams usually possess relatively large velocities and, because of Eq. (2), can cause a large pertinent effective basal shear stress acting on the bed load. These rapid flows further mobilize the sediments

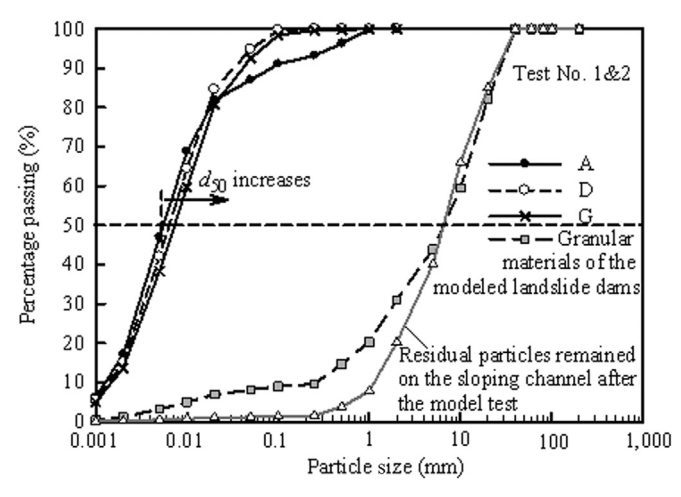


Fig. 10. Particle size distribution of the sampled debris flows for Test Nos. 1 and 2. Lines A, D, and G represent the front debris flow sampled at these respective points along the channel.

deposited on the bed from the collapsed landslide dams, and these sediment flows entrain yet more solid particles (cf. Eq. (1)) and gradually transform into hyperconcentrated flows or even debris flows. Fig. 8d shows a geomorphologic view after the modeling test, evincing deep pools and significant erosion at the front side (downstream face) of the originally constructed landslide dams, while the rock dams remain relatively stable.

3.3. Cascading failure of landslide dams due to overtopping and erosion

For experimental Test No. 3, cascading landslide dams of limited size were constructed and distributed along sloping channel II on the deposition fan of Chaqing Gully. Such landslide dams are mostly triggered by local slope failures or small rock avalanches with relatively short run-out distances. Thus, they usually stand aside a channel bank and partially block the sloping channel. Similar to the failure modes of the landslide dams in Tests No. 1 and No. 2, the landslide dams partially blocking the channel river in Test No. 3 also mostly failed due to overtopping. In the test, most of the flow is blocked when the front flow passes through the narrow cross-sections constructed by the landslides and cliffs (see the channel sidewalls in Table 1), and the water levels naturally rise behind the dams. Once the flows overtop the first landslide dam and a failure occurs, a strong wave (high speed) moves downwards (Fig. 11a), crushing the other downstream landslide dams and causing large breaches (Fig. 11b and c). In addition to the overtopping water flows, lateral erosion of the landslide dams (parallel to the flow direction) also accounts for the development of breaches and major failures of the dam bodies. Also, we can see from Fig. 11a-c that when the accelerating flow crushes the downstream cluster of landslide dams at relatively high velocities. the resulting landslide dams failures are quite rapid. The front velocity and discharge gradually increase in conjunction with the cascading failures of the landslide dams in a fashion similar to the results of Test No. 1 and No. 2 (Fig. 12). Moreover, the accelerating flow causes both an increase in particles size and in the amount of granular material entrained by the front flow, as shown in Fig. 13.

After the test, the geomorphologic topology was imaged using a 3D laser scanner and the resulting channel shape compared to that of the original sloping channel (Fig. 11d). In contrast to piping water flows which induce more erosion of bed sediments, the uplifted channel bed in Fig. 14 demonstrates that the cascading landslide dam failures in Test No. 3 directly deposited large quantities of sediments before the constructed landslide dams (at the toe of the downstream face). The figure also shows a significant amount of sedimentation and aggradation of coarse sediments on the bed surface. In addition, the masses of the deposited granular materials on the channel bed which came from the three upstream landslide dams (i.e., LD-1, LD-2, and LD-3 in Fig. 14) are much larger than the masses deposited from the downstream landslide dams (i.e., LD-4 and LD-5). This result suggests that erosion and deposition of sediments on the channel bed develop in conjunction with the cascade of landslide dam failures. Moreover, the flow velocity and discharge gradually increase after each successive dam failure, which usually induces more entrainment of solids into the flow (cf. Eqs. (1) and (2)). After the flow velocity fully develops after the first few landslide dam failures, erosion by the flow dominates the resulting deposition of solids after the failures of the last two landslide dams (LD-4 and LD-5). The variation in uplifted channel bed surface at the toes of the landslide dams also proves that the scale of the flow can be significantly influenced by the cascading failure of landslide dams. In general, the test resulted in a gradually enlarged downstream flow (cf. Fig. 12). The three modeling tests (Nos. 1, 2 and 3) further illustrate that clusters of landslide dams can also act as a primary control on channel morphology and longitudinal river profiles in a manner similar to single large landslide events (cf. Ouimet et al., 2007) by reducing or even enhancing a river's incision efficiency. However, the effects of cascading landslide dam failures are obviously more complicated.

A physical breach model for landslide dams has been proposed by Chang and Zhang (2010), which involves breach evolution, erosion mechanics, and breach hydraulics. The observed failure process of the landslide dams in both Test No. 1 and Test No. 2 does prove that the assumed evolution of the breach, at least in relation to the side slope collapse and flow conditions proposed by Chang and Zhang (2010), is correct for large landslide dams fully blocking a sloping channel. The proposed model also explains the two-stage failure process of clusters of landslide dams partially blocking a channel (i.e., Test No. 3). In the first stage of erosion, our experiments show that the erosion of the landslide dams starts at the side slopes below the water level, which causes the side slopes above the water level to collapse. The erosion direction is mostly perpendicular to the previous side slope, as shown in Fig. 15 from Line 1 to Line 2. This process continues until the side slopes reach a critical value α_c , which can be determined through a slope stability analysis as illustrated by Chang and Zhang (2010). Both the breach depth and breach bottom width gradually increase during this process. After the side slopes reach this critical angle, the sides recede laterally while maintaining the same critical angle α_c as erosion continues into stage two (Fig. 15, from Line 2 to Line 3). This process stops when the shear stress applied by the overtopped water flow cannot overcome the erosion resistance of the landslide dam soils. During this second stage, the breach erosion depth remains constant (not considering the channel bed erosion), whereas the breach top width and bottom width increase. Most of the landslide dams in the experiments follow the process described above. The difference in the process for Tests No. 1, 2, and 3 was that when the upstream discharge was relatively small, a dammed lake usually formed behind the first landslide dam. In this case, infiltration and slope failure rather than direct erosion become the main causes of breach development.

4. Conclusions

The dynamic process of flows along a sloping channel was investigated through the experimental study of cascading landslide dam failures in Zhouqu, China by analyzing the failure modes caused by upstream flows of different constructed landslide dams. The results from three different model tests illustrate that upland flows can indeed cause a cascading failure of downstream landslide dams for virtually any type of constructed landslide dam. These dam failures can all significantly enhance flow discharge, despite their resulting from different failure modes and mechanisms. From analysis of the three test flows, we can further conclude the following:

(1) For fully blocked sloping channels, the upstream flow initially raises the water level and inundates the upstream area behind the landslide dams. Overtopping of the water flow suddenly causes the failure of the crest of such landslide dams and then gently mobilizes the dam body. Instability develops from the crest to the toe of the dams, and more and more coarse soil particles are entrained into the flows. Rapid waves resulting from the failures of landslide dams were observed in the tests, which moved downwards and caused cascading failures of other downstream landslide dams. Once the flow successively crushes a landslide dam in this manner, more granular material erodes away from the dam and mixes with the flow, resulting in enlarged flow discharges.

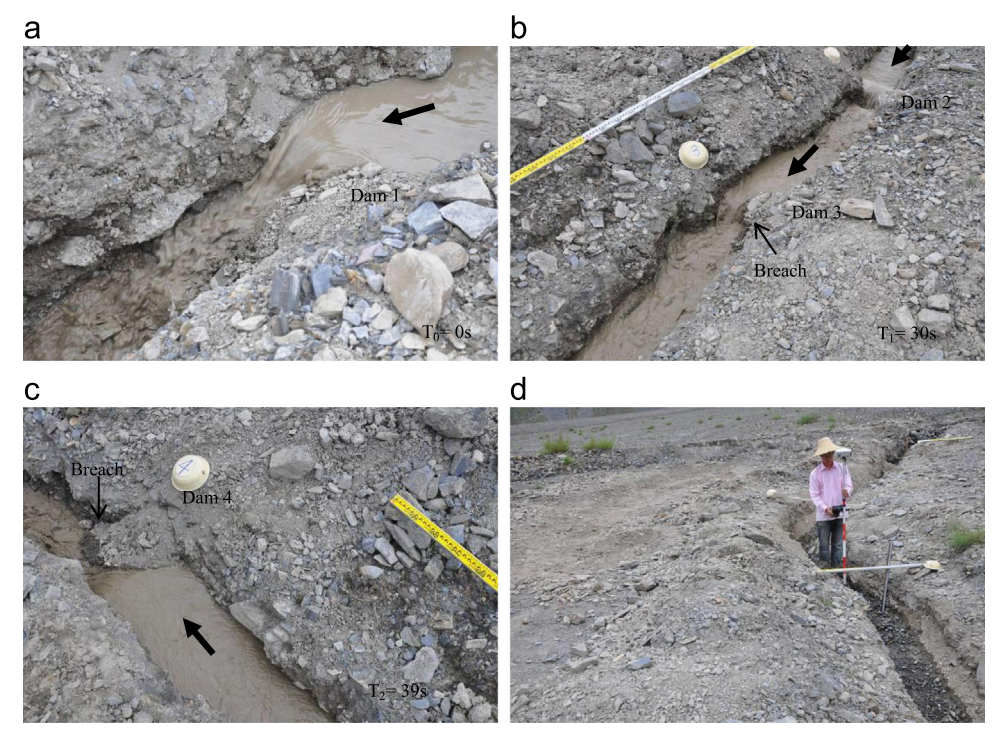


Fig. 11. Evolution of the failure process of the soil dams in model Test No. 3.

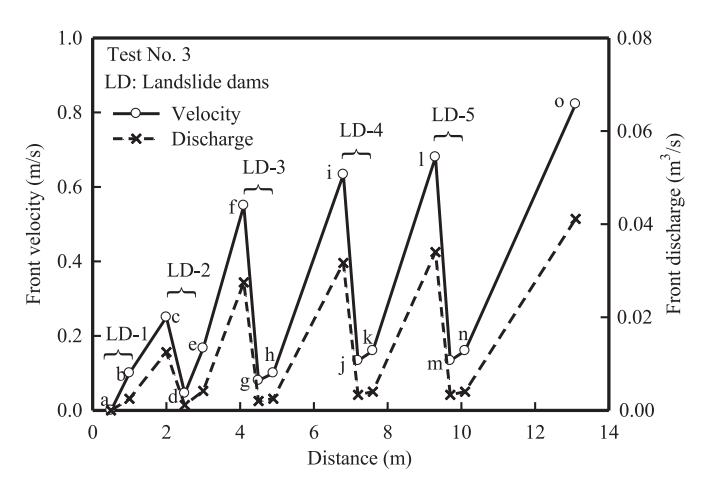


Fig. 12. Variation in the measured velocity and discharge of the front debris flow along the sloping channel for Test No. 3.

- (2) Landslide dams that fully block a sloping channel with rock dams can be rapidly crushed by upstream flows. Usually, this dynamic process is quite rapid, even for relatively small upstream discharges. Besides the overtopping of water flows that gradually causes instability inside a landslide dam, piping also occurs through the loosely contacted particles inside rock dams. The front flows gradually accelerate in conjunction with the cascading landslide dam failures, and the high crushing speeds make the downstream dams lose strength completely. This further explains the significant erosion of bed sediments in front of such landslide dams (downstream face); the soil particles are directly entrained into the flows, and cause an increase in the discharge of solid–water mixtures (debris flows).
- (3) Landslide dams of limited scale and which only partially block a sloping channel can still fail in a cascading mode. Upstream flows transport through the narrow gap constructed by landslide dams between the dam and the channel sidewalls and cause dam failures. The flow accelerated by one such failure then induces

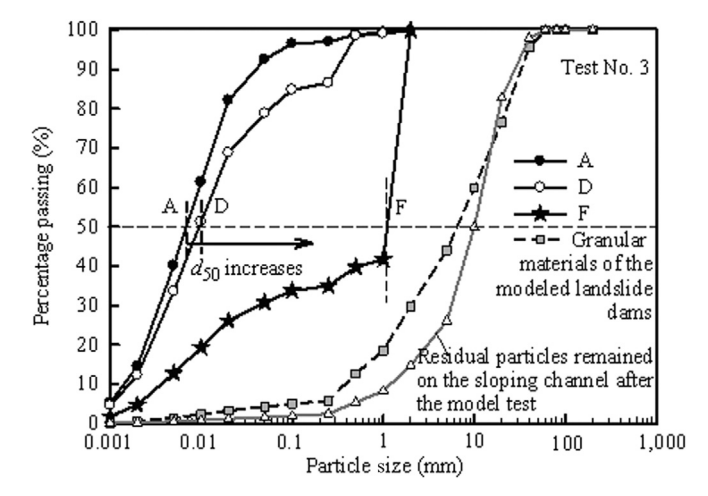


Fig. 13. Particle size distribution of the sampled debris flows for Test No. 3. Lines A, D, and F represent the front debris flow sampled at the respective positions along the channel.

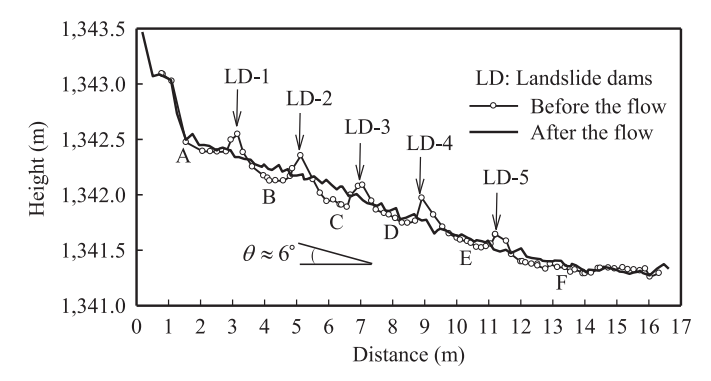


Fig. 14. Comparison of channel geomorphology before and after the cascading landslide dam failures in Test No. 3.

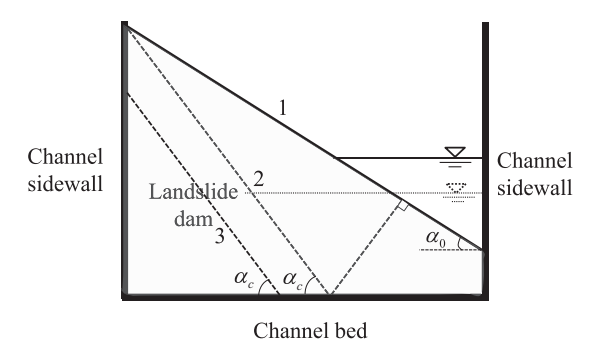


Fig. 15. Breach enlargement and landslide dam failure process.

rapid and significant erosion of subsequent landslide dams further down the channel. The flow scale gradually increases to the point where the flow can crush downstream landslide dams through kinetic energy, while developed breaches inside the landslide dams also accelerate their rapid failure and erosion.

(4) The three model tests further illustrate that most clusters of landslide dams closely distributed in a sloping channel can be induced to fail in a cascading fashion by upstream flows, and thus significantly increase the size of downstream destructive (debris) flows. Such clusters of landslide dams can also act as a primary control on channel morphology and longitudinal river profile in a manner similar to large single landslide events, reducing or even enhancing a river's incision efficiency. However, it is obviously much more complicated to predict the effect of a cascading series of smaller dam failures compared to predicting the effects of the failure of a single large dam.

Acknowledgments

The authors acknowledge financial support from the Key Research Program of the Chinese Academy of Sciences (Grant no. KZZD-EW-05-01), the National Natural Science Foundation of China (NSFC) (Grant no. 41201012, 41371038), and the Hundred Young Talents Program of the Institute of Mountain Hazards and Environment (Grant no. SDSQB-2013-01). The great help from Dongchuan Debris Flow Observation and Research Station is also gratefully acknowledged. Finally, the authors thank the two anonymous reviewers of this paper for the detailed remarks and helpful discussions.

References

Carrivick, J. L. (2010). Dam break – outburst flood propagation and transient hydraulics: a geosciences perspective. *Journal of Hydrology*, 380(3-4), 338–355.
 Chang, D. S., & Zhang, L. M. (2010). Simulation of the erosion process of landslide dams due to overtopping considering variations in soil erodibility along depth. *Natural Hazards and Earth System Science*, 10(4), 933–946.

Chang, D. S., Zhang, L. M., Xu, Y., & Huang, R. Q. (2011). Field testing of erodibility of two landslide dams triggered by the 12 May Wenchuan earthquake. *Landslides*, 8(3), 321–332.

Chartrand, S. M., Jellinek, M., Whiting, P. J., & Stamm, J. (2011). Geometric scaling of step-pools in mountain streams: observations and implications. *Geomorphology*, 129(1–2), 141–151.

Chen, C. C., Chen, T. C., Yu, F. C., & Hung, F. Y. (2004). A landslide dam breach induced debris flow—a case study on downstream hazard areas delineation. *Environmental Geology*, 47, 91–101.

Cleary, P. W., & Prakash, M. (2004). Discrete-element modelling and smoothed particle hydrodynamics: potential in the environmental sciences. *Philosophical Transactions of the Royal Society A: Mathematical, Physical and Engineering Sciences*, 362(1822), 2003–2030.

Corominas, J., & Moya, J. (2008). A review of assessing landslide frequency for hazard zoning purposes. Engineering Geology, 102(3-4), 193-213.

Costa, J. E. (1985). Floods from dam failures (pp. 85–560). United States geological survey open-file report. Costa, J. E., & Schuster, R. L. (1988). Formation and failure of natural dams. Bulletin of the Geological Society of America, 100(7), 1054–1068.

Crosta, G. B., & Clague, J. J. (2009). Dating, triggering, modelling, and hazard assessment of large landslides. *Geomorphology*, 103(1), 1-4.

Cui, P., Zhu, Y. Y., Han, Y. S., Chen, X. Q., & Zhuang, J. Q. (2009). The 12 May Wenchuan earthquake-induced landslide lakes: distribution and preliminary risk evaluation. *Landslides*, 6, 209–223.

Davies, T. R. H. (1986). Large debris flows: a macro-viscous phenomenon. *Acta Mechanica*, 63(1–4), 161–178.

Dong, J. J., Tung, Y. H., Chen, C. C., Liao, J. J., & Pan, Y. W. (2009). Discriminant analysis of the geomorphic characteristics and stability of landslide dams. *Geomorphology*, 110, 162–171.

Dong, J. J., Li, Y. S., Kuo, C. Y., Sung, R. T., Li, M. H., Lee, C. T., et al. (2011). The formation and breach of a short-lived landslide dam at Hsiaolin village, Taiwan – part I: post-event reconstruction of dam geometry. *Engineering Geology*, 123 (1–2), 40–59.

Ermini, L., & Casagli, N. (2003). Prediction of the behaviour of landslide dams using a geomorphological dimensionless index. *Earth Surface Processes and Landforms*, 28(1), 31–47.

Gomez, B., & Church, M. (1989). An assessment of bed load sediment transport formulae for gravel bed rivers. Water Resources Research, 25, 1161–1186.

Hewitt, K. (1998). Catastrophic landslides and their effects on the Upper Indus streams, Karakoram Himalaya, northern Pakistan. *Geomorphology*, 26, 47–80.

Hovius, N., Stark, C. P., & Allen, P. A. (1997). Sediment flux from a mountain belt derived from landslide mapping. *Geology*, 25, 231–234.

Hovius, N., Stark, C. P., Tutton, M. A., & Abbott, L. D. (1998). Landslide-driven drainage network evolution in a pre-steady-state mountain belt: Finisterre Mountains, Papua New Guinea. Geology, 26, 1071–1074.

Hsu, Y. S., & Hsu, Y. H. (2009). Impact of earthquake-induced dammed lakes on channel evolution and bed mobility: case study of the Tsaoling landslide dammed lake. *Journal of Hydrology*, 374(1–2), 43–55.

Iovine, G., Gregorio, S. D., Sheridan, M. F., & Miyamoto, H. (2007). Modelling, computer-assisted simulations, and mapping of dangerous phenomena for hazard assessment. *Environmental Modelling and Software*, 22(10), 1389–1391.

Julien, P. Y. (1995). Erosion and sedimentation. New York, NY: Cambridge Univ. Press. Keefer, D. K. (1999). Earthquake-induced landslides and their effects on alluvial fans. Journal of Sedimentary Research, 69(1), 84–104.

King, J., Loveday, I., & Schuster, R. L. (1989). The 1985 Bairaman landslide dam and resulting debris flow. *Quarterly Journal of Engineering Geology*, 22(4), 257–270.
 Korup, O. (2002). Recent research on landslide dams – a literature review with special

Korup, O. (2002). Recent research on landslide dams – a literature review with special attention to New Zealand. Progress in Physical Geography, 26(2), 206–235.
Korup, O. (2004). Geomorphometric characteristics of New Zealand landslide dams.

Engineering Geology, 73, 13–35.
Korup, O. (2005). Geomorphic hazard assessment of landslide dams in South

Westland, New Zealand: fundamental problems and approaches. *Geomorphology*, 66(1–4), 167–188.

Korup, O., Densmore, A. L., & Schlunegger, F. (2010). The role of landslides in mountain range evolution. *Geomorphology*, 120(1–2), 77–90.

Korup, O., McSaveney, M. J., & Davies, T. R. H. (2004). Sediment generation and delivery from large historic landslides in the Southern Alps, New Zealand. *Geomorphology*, 61(1–2), 189–207.

Korup, O., Strom, A. L., & Weidinger, J. T. (2006). Fluvial response to large rock-slope failures—examples from the Himalayas, the Tien Shan, and the New Zealand Southern Alps. *Geomorphology*, 78, 3–21.

Li, M. H., Hsu, M. H., Hsieh, L. S., & Teng, W. H. (2002). Inundation potentials analysis for Tsao-Ling landslide lake formed by Chi-Chi earthquake in Taiwan. *Natural Hazards*, 25, 289–303.

Li, M. H., Sung, R. T., Dong, J. J., Lee, C. T., & Chen, C. C. (2011). The formation and breaching of a short-lived landslide dam at Hsiaolin Village, Taiwan – part II: simulation of debris flow with landslide dam breach. *Engineering Geology*, 123 (1–2), 60–71.

Montgomery, D. R., Panfil, M. S., & Hayes, S. K. (1999). Channel-bed mobility response to extreme sediment loading at Mount Pinatubo. *Geology*, *27*(3), 271–274.

Nandi, A., & Shakoor, A. (2009). A GIS-based landslide susceptibility evaluation using bivariate and multivariate statistical analyses. *Engineering Geology*, 110, 11–20.

Nezu, I., Kadota, A., & Nakagawa, H. (1997). Turbulent structure in unsteady depthvarying open-channel flows. *Journal of Hydraulic Engineering*, 123(9), 752–762.

Ouimet, W. B., Whipple, K. X., Royden, L. H., Sun, Z., & Chen, Z. (2007). The influence of large landslides on river incision in a transient landscape: eastern margin of the Tibetan Plateau (Sichuan, China). *Bulletin of the Geological Society of America*, 119(11–12), 1462–1476.

Peng, M., & Zhang, L. M. (2012). Breaching parameters of landslide dams. *Landslides*, 9(1), 13–31.

Ralston, D. C. (1987). Mechanics of embankment erosion during overflow. In R. M. Ragan (Ed.), Proceedings of the 1987 national conference on hydraulic engineering (pp. 733–744). New York: American Society of Civil Engineers.

Plafker, G., & Ericksen, G. E. (1978). Nevado Huascaran avalanches, Peru. In: B. Voight (Ed.), New York: Elsevier.

Richardson, E. V., Simons, D. B., Julien, P. Y. (1990). *Highways in the river environment*. U.S. Dept. of Transportation, Federal Highways Administration.

Scott, K. M., Vallance, J. W., & Pringle, P. T. (1995). Sedimentology, behavior, and hazards of debris flows at Mount Rainier (p. 56) Washington: U.S. Geol. Surv. Prof. Pap. 1547.

- Shields, A. (1936). Änwendung der Ahnlichkeitsmechanik und der Turulenzforschung auf die Geschiebebewegung. 26. Berlin: Mitteilungen der Preussischen Versuchsanstalt für Wasserbau und Schiffbau.
- Strasser, M., & Schlunegger, F. (2005). Erosional processes, topographic lengthscales and geomorphic evolution in arid climatic environments: the "Lluta collapse", northern Chile. *International Journal of Earth Sciences*, 94, 433–446.
- Swanson, F. J., Oyagi, N., & Tominaga, M. (1986). Landslide dams in Japan. In: R. L. Schuster (Ed.), *Landslide dams: processes, risk, and mitigation*, Vol. 3 (pp. 131–145). Japan: American Society of Civil Engineers, Geotechnical Special Publication.
- Tang, C., Rengers, N., Van Asch, T. W. J., Yang, Y. H., & Wang, G. F. (2011). Triggering conditions and depositional characteristics of a disastrous debris flow event in Zhouqu city, Gansu Province, northwestern China. *Natural Hazards and Earth System Science*, 11(11), 2903–2912.
- Thompson, D. M., Nelson, J. M., & Wohl, E. E. (1998). Interactions between pool geometry and hydraulics. *Water Resources Research*, 34(12), 3673–3681.

- Walder, J. S., & O'Connor, J. E. (1997). Methods for predicting peak discharge of floods caused by failure of natural and constructed earthen dams. *Water Resources Research*, 33(10), 2337–2348.
- Wang, Z., Cui, P., Yu, G., & Zhang, K. (2012). Stability of landslide dams and development of knickpoints. *Environmental Earth Sciences*, 65(4), 1067–1080.
- Wang, Z. Y., & Zhang, K. (2012). Principle of equivalency of bed structures and bed load motion. *International Journal of Sediment Research*, 27(3), 288–305.
- Wilcox, A., & Wohl, E. E. (2007). Field measurements of three-dimensional hydraulics in a step-pool channel. *Geomorphology*, 83, 215–231.
- Yalin, M. S. (1971). Theory of hydraulic models. Oxford: Macmillan.
- Yu, B., Yang, Y. H., Su, Y. C., Huang, W. J., & Wang, G. F. (2010). Research on the giant debris flow hazards in Zhouqu county, Gansu Province on August 7, 2010. *Journal of Engineering Geology*, 4, 437–444.
- Zhao, Y. C., & Cui, C. G. (2010). A study of rainstorm process triggering Zhouqu extremely mudslide on 8 August 2010. *Torrential Rain and Disasters*, 9, 289–295 in Chinese